SUPPORTING INFORMATION

Molecular mechanism for inhibition of twinfilin by phosphoinositides

Markku Hakala[1], Maria Kalimeri[2], Giray Enkavi[3], Ilpo Vattulainen[2,3,4], Pekka Lappalainen[1]

[1]Institute of Biotechnology, University of Helsinki, Finland
[2]Department of Physics, Tampere University of Technology, Tampere, Finland
[3]Department of Physics, University of Helsinki, Helsinki, Finland
[4]MEMPHYS – University of Southern Denmark, Odense, Denmark

Contents:

SUPPORTING MOLECULAR DYNAMICS SIMULATION RESULTS

The twinfilin C-terminal tail has transient structure in helical and turn conformations. The structure offlexible carboxy-terminal tail (residues 317-350) of twinfilin has remained unknown due to its flexible nature. However, secondary structure prediction algorithms (1-3) indicate possible helical or beta sheet structures at the regions 320-323 and 334-340 (data not shown). To probe the propensity of the twinfilin tail for well- defined secondary structure, we first performed unbiased MD simulations of the C-terminal tail region detached from the rest of the protein. We studied three different membrane-free systems in water (Table S1), with different starting conformations for the tail: random coil (system 1), antiparallel β-sheet (system 2) or α- helical (system 3). The coil-based simulation showed highly transient structures with minor helical and beta sheet content. Most notably, during the second half of the simulation, the proline-containing regions K325- G328 and G341-E344 remained in a turn conformation (Movie S1). The turn conformation between the residues G341 and E344 appeared also in simulations that started with either β-sheet or α-helical conformation. Interestingly, for the helix-based simulation, the middle region of the tail (K332-I339) remained in a folded conformation throughout all explored timescales in every simulation (Fig. S2 A, Movie S2), while the β-sheet starting conformation maintained the β-sheet structure in a much smaller region and was largely unfolded (Fig. S2 D). Results of additional Replica Exchange Solute Tempering simulations (system 4) did not indicate substantial folding (data not shown). Overall, our simulations indicated that the C-terminal tail region to be mainly unfolded, with transient structures consistent with α-helical and turn conformations.The simulation results on the transient structures found in the twinfilin C-terminal tail were used to construct a more complete description for twinfilin. To build systems 5 and 7 (Table S1), in other words the C-terminal ADF-H domain attached to the 34-residue tail in either α-helical or β-sheet structure, we performed clustering analysis on the concatenated trajectories of systems 3 and 2, respectively. The N-terminal ADF-H domain was not included in these experiments to reduce system size. For the clustering analysis, we used the leader follower algorithm (4,5), we used the root-mean square deviation (RMSD) of carbon backbone atoms as a collective variable. For the helical case, the protein trajectory was aligned on the carbon backbone atoms of residues K332-I339 (i.e., the middle region that remained folded throughout all simulations) and, with a cutoff of 1.5 nm, we obtained three different clusters (see conformations of centroids in the top of Fig. S2 A). For the β- sheet (Fig. S2 D-E), the alignment was done on the carbon backbone atoms of residues K333-I339, and with a cutoff of 1.5 nm we obtained one very populated cluster and five less populated ones. We used the most prevalent cluster to reconstruct the C-terminal domain together with the tail (system 7).

SUPPORTING TABLES

Table S1: Descriptions of simulated systems and the simulation details

System number	System type	Starting tail conformation	No. of lipids in upper leaflet / lower leaflet = PC:PE:PS:PI(4,5)P_2/PC:PE:PS	No. of repeats	No. Of waters	Initial distance from membrane surface* (nm)	Simulation time (ns)	Simulation type
1	C-ter tail [A]	Random coil	–	1	47189	-	320	Unbiased
2	C-ter tail [A]	Beta sheet	–	2	19567, 19590	-	350	Unbiased
3	C-ter tail [A]	Helical	–	4	45671, 45671, 45671, 45671	-	160, 200, 240, 400	Unbiased
4	C-domain with tail [B]	Random coil	–	1	31020	-	100	Replica exchange solute tempering
5	C-domain with tail [B]	Helical	88:40:35:23 / 109:41:34	6	50797, 50793, 50798, 51091, 51101, 51091	6.0, 5.9, 2.8**, 5.2, 3.5, 5.2	450, 400, 700, 160, 70, 200	Unbiased
6	C-domain with tail [B]	Random coil	88:40:35:23 / 109:41:34	2	50703, 50760	4.5, 4.8	570, 230	Unbiased
7	C-domain with tail [B]	Beta sheet	88:40:35:23 / 109:41:34	3	51193, 51168, 51168	5.3, 5.0	300, 300, 300	Unbiased
8	C-ter tail [A]	Random coil	88:40:35:23 / 109:41:34	1	36095	3.5	230	Unbiased
9	C-ter tail [A]	Helical	88:40:35:23 / 109:41:34	4	36138, 36138, 36138, 36138	4.2, 4.2, 4.2, 4.2	100	Unbiased
10	C-domain without tail [C]	-	88:40:35:23 / 109:41:34	6	35091, 35087, 35098, 35104, 35076, 35076	4.3, 4.0, 5.1, 5.1, 4.2, 4.2	400, 260, 270, 300, 330, 280	Unbiased
11	C-domain with neutralized tail [B]	Helical	88:40:35:23 / 109:41:34	6	50793, 50793, 50793, 50793, 50793, 50793	6.2, 6.3, 6.8, 7.2, 7.4, 6.0	600, 600, 600, 600, 600, 600	Unbiased

[A] 34-residue long C-terminal tail of 2HD7 (i.e., residues 317-350).

[B] 176-residue long C-domain of 2HD7 including the last 34-residue long tail.

[C] 142-residue long C-domain of 2HD7 without the last 34-residue long tail.

* Distance along membrane normal direction between the center of mass of the protein and the center of mass of the phosphorus atoms of the PIP-rich bilayer.

** Both the average and the minimum distance between the protein and the PIP-rich bilayer were purposefully small with the putative binding site of the protein facing away from the bilayer. During the course of 700 ns, the protein twisted around and reproduced, once more, the binding site observed in the previous two simulations.

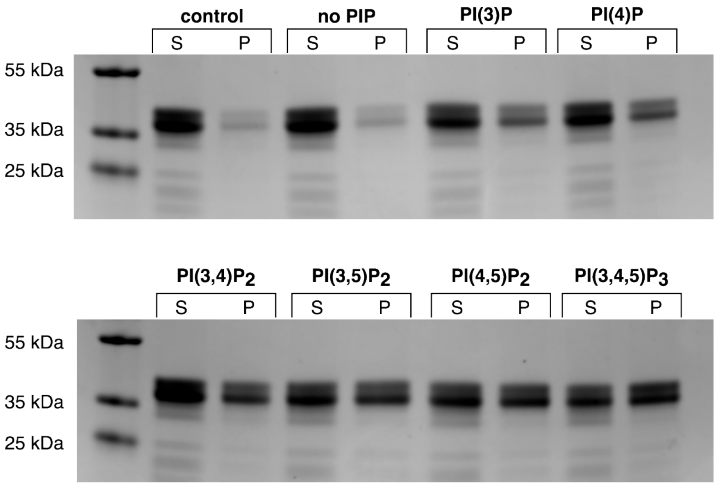

Figure S1. Twinfilin has higher affinity towards more charged phosphoinositides. A representative gel image of a lipid vesicle co-sedimentation assay on wild-type full length twinfilin (40 kDa). S=supernatant, P=pellet. Protein concentration was 2 μM and total concentration of lipids was 500 μM. The lipid composition was POPC:POPE:POPS:PIP= 55:20:20:5, except in "no PIP" sample, were lipid composition was POPC:POPE:POPS= 60:20:20.

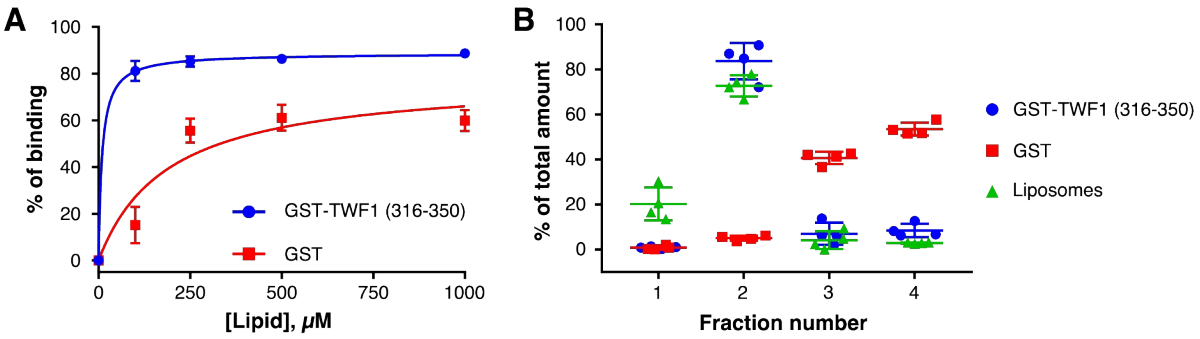

Figure S2. The isolated tail of twinfilin interacts with lipids. (A) A vesicle co-sedimentation assay performed on purified GST and GST-twinfilin tail fusion protein. The final protein concentration was 2 μM, and the lipid concentration varied from 0 to 1000 μM. The lipid composition was POPC:POPE:POPS:PI(4,5)P2 = 50:20:20:10. Data points are a mean of four individual experiments. Error bars represent standard deviations. (B) A vesicle co-flotation assay performed for the same proteins. The final protein and lipid concentrations were 1 μM and 1 mM, respectively. The lipid composition was POPC:POPE:POPS:PI(4,5)P2 = 50:20:20:10. Data are shown as individual data points and as the mean from four experiments. Error bars represent standard deviations.

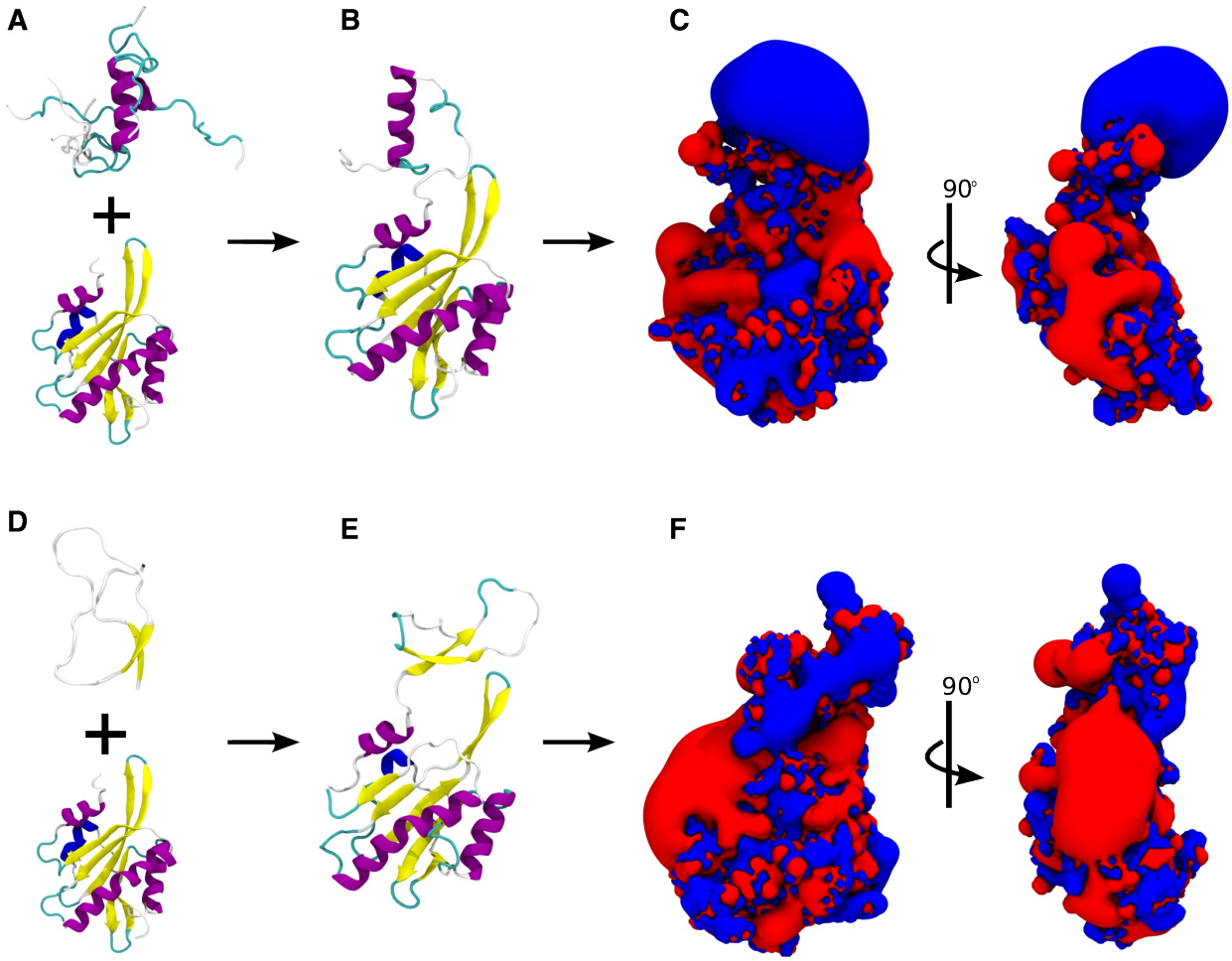

Figure S3. The structure and electrostatics of the twinfilin tail. (A) Most prevalent α-helical conformation of the C-terminal tail of twinfilin as found by cluster analysis performed on atomistic MD simulation in water (top). C-terminal ADF-H domain is also shown (bottom). (B) C-terminal tail in its most stable helix-containing conformation shown attached to the C-terminal ADF-H domain. (C) Electrostatic potential isocontours of the C-terminal ADF-H domain and the tail region in the α-helix-containing conformation are shown for -1.5 kT/e (red) and +1.5 kT/e (blue). (D) The β-sheet conformation of the tail region (top) of twinfilin and the structure of C-terminal ADF-H domain (bottom). (E) The tail in β-sheet conformation attached to the C-terminal ADF-H domain of twinfilin. (F) Electrostatic potential isocontours of the tail in β-sheet conformation and C-terminal ADF-H domain of twinfilin are shown for -1.5 kT/e (red) and +1.5 kT/e (blue).

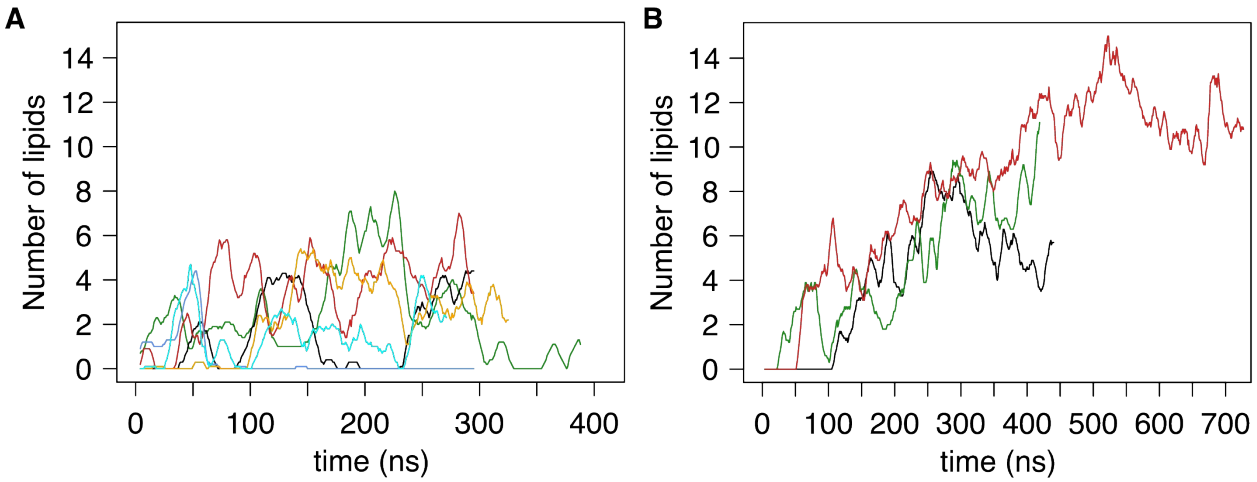

Figure S4. The binding affinity of lipids and twinfilin with and without the tail region. Number of lipids hydrogen-bonded to any residue of twinfilin without tail (A) and with tail (B). Each line graph represents individual simulation experiment.

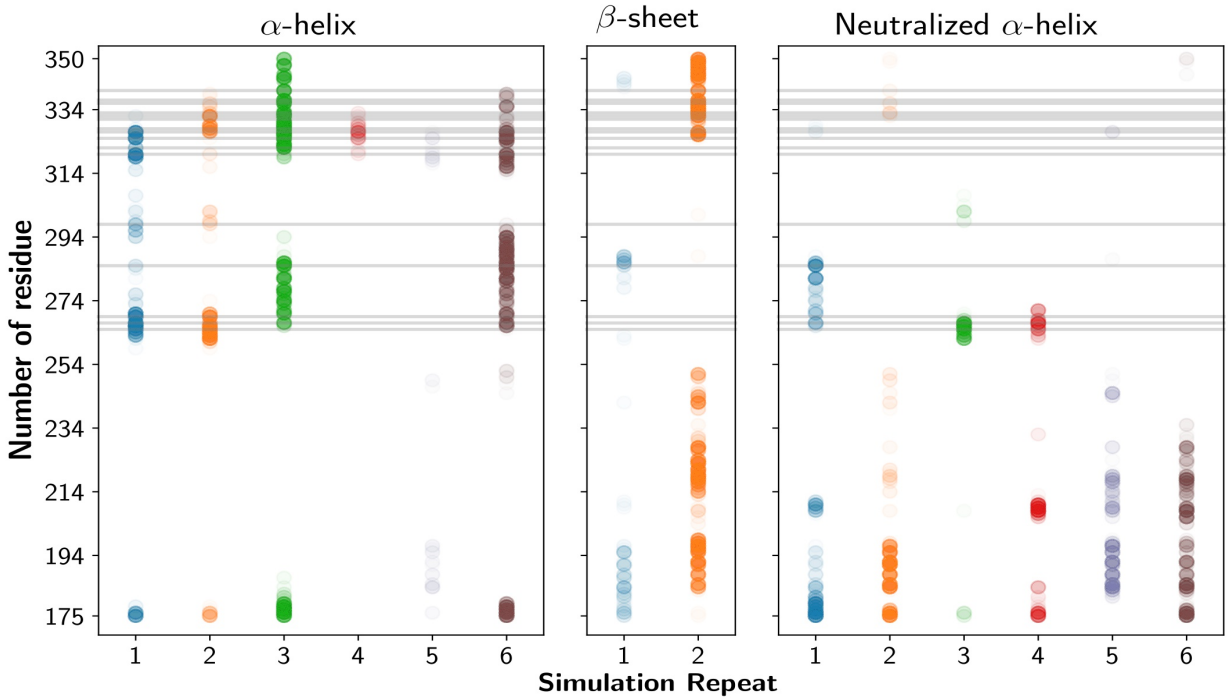

Figure S5. Contact frequency between lipids and twinfilin. The residue-residue contacts (calculated with an atom-pair cut-off of 5 Å) between the protein and lipids calculated over the last 50 ns. The opacity of the circular marks is proportional to the frequency of contacts with a particular residue. Positions of the residues that strongly interact with the membrane (K320, S322, K325, K327, G328, G331, K332, R333, R336, R337, R340 in the C-terminal tail and S265, R267, R269, R285, D298 in the ADF-H domain) are marked with vertical lines. Simulation repeats and systems where no contact is observed are not shown. The reproducibility of the membrane contacting residues particularly in the C-terminal tail is enhanced in α-helical tail (system 5) conformation when compared to β-sheet tail (system 7) conformation and neutralized α-helical tail (system 11).

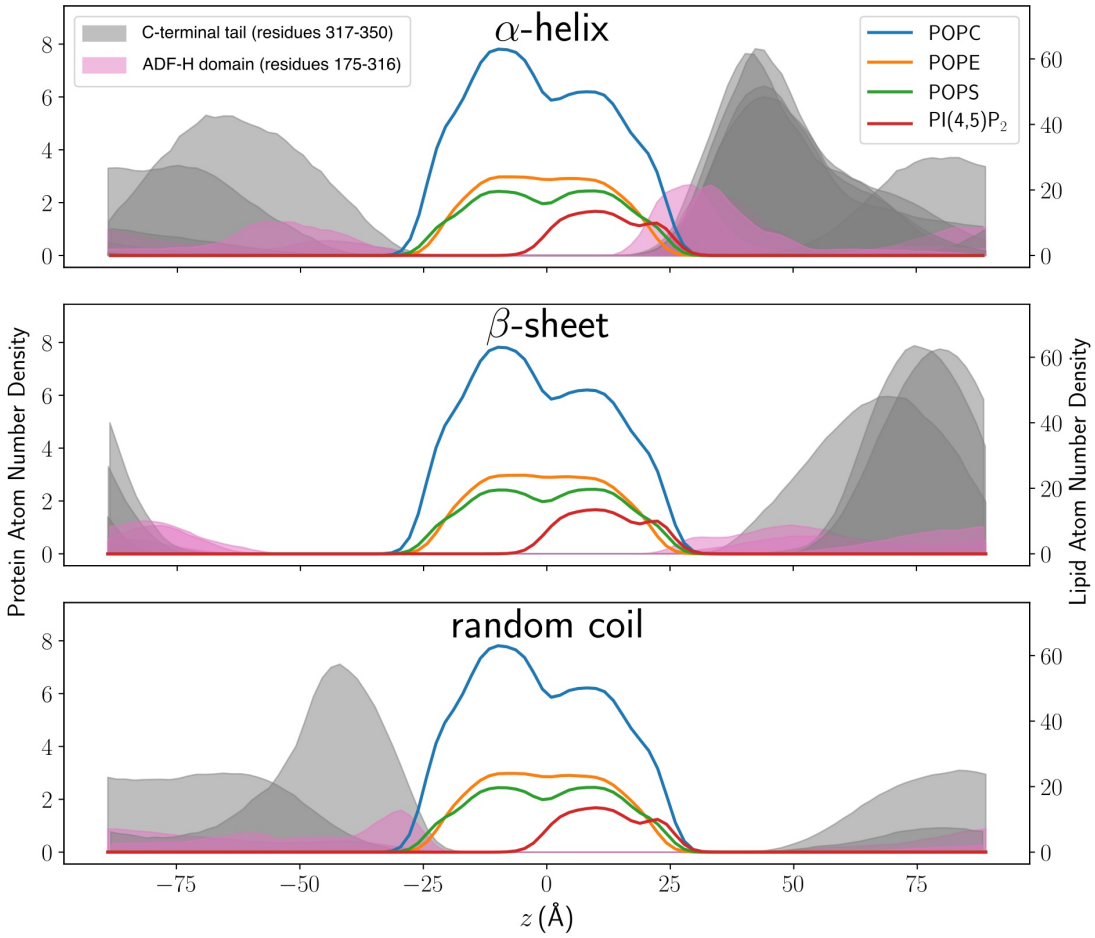

Figure S6. Atom number densities as a function of z-axis (membrane normal) estimated from simulations with α-helical (top panel, system 5), β-sheet (middle panel; system 7) and random coil (bottom panel; system 8)) C-terminal tail conformations. In all three systems, the average atom number densities of the lipids over all repeats (see Table S1) are shown in lines (center of the membrane is placed at z=0). The atom number densities of the C-terminal and N-terminal regions of the protein are shown semi-transparently (grey and pink, respectively) for each repeat performed for the system, separately. Strong overlap between the C- and N-terminal regions of the protein and PI(4,5)P2-containing leaflet (red line) is only seen when C-terminal tail is in α-helical (top panel, system 5) conformation. In other conformations of the tail (β-sheet (middle panel; system 7) and random coil (bottom panel; system 8)), protein either does not bind the membrane or localizes to non-PI(4,5)P2-containing leaflet.

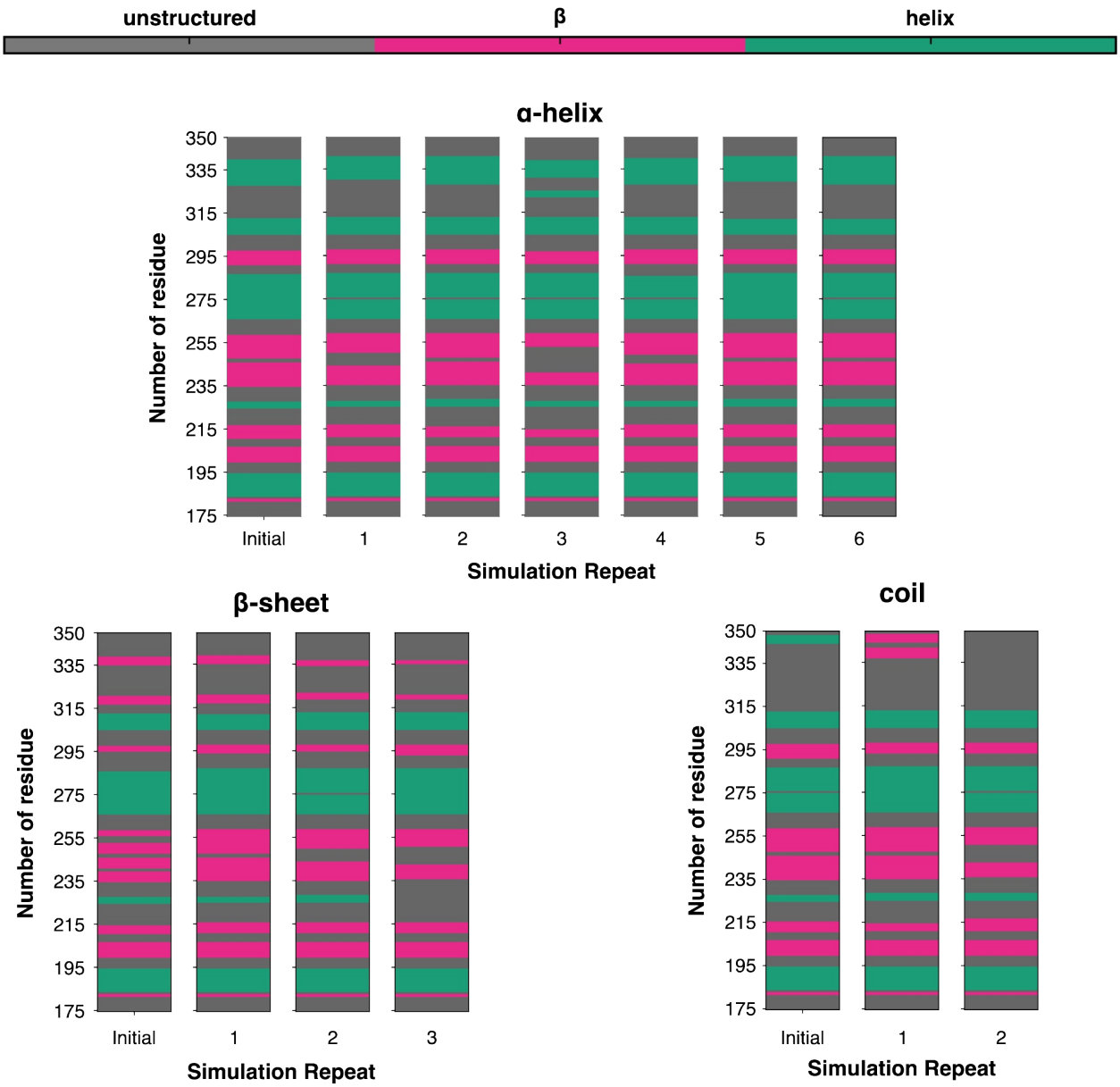

Figure S7. The conformation changes in the secondary structure of twinfilin upon lipid-binding. The secondary structure content of twinfilin was calculated using DSSP (6-7) for the initial and the last 50 ns of each simulation repeat with C-terminus initially in α-helix (system 5; upper panel), β-sheet (system 7; lower left panel), and random coil structures (system 6; lower right panel). The DSSP secondary structures were further grouped into helix (α-helix, 3-helix, or 5-helix), β (β-sheet or β-bridge), and unstructured (rest) categories for simplicity. The consensus secondary structure over all repeats in the first 50 ns (10 frames × Number of repeats) and that over the last 50 ns (10 frames) for each repeat are shown.

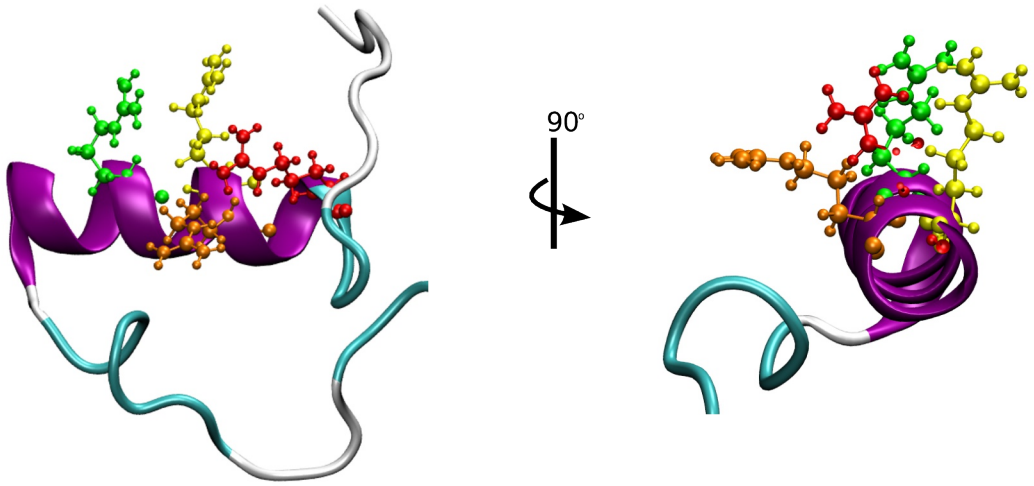

Figure S8. A periodical pattern of arginines in the twinfilin tail. Positively charges arginines R333 (green), R336 (yellow), R337 (orange) and R340 (red) follow pattern of n,n+3 and n,n+4 to form a surface of positive charge on one side of the helix for lipid interaction, thus supporting the proposed helical structure in the tail.

SUPPORTING MOVIE LEGENDS

MOVIE S1.
Proline-rich regions generate two turns in the C-terminal tail of twinfilin-1 (system 1).

MOVIE S2.
The middle region of the twinfilin tail remains in a α-helical conformation (system 3).

MOVIE S3.
Twinfilin binds efficiently the PI(4,5)P2-rich membrane leaflet (system 5). A simulation (400 ns) of twinfilin with the tail in a α-helical conformation and membranes with (top) the PI(4,5)P2-rich and (bottom) the PI(4,5)P2-free leaflet. Leaflets are periodic images of the asymmetric lipid bilayer.

MOVIE S4.
Twinfilin tail in a coil conformation does not bind the PI(4,5)P2-rich membrane leaflet (system 6). A simulation of twinfilin with the tail in a coil conformation and membranes with (top) the PI(4,5)P2-rich and (bottom) the PI(4,5)P2-free leaflet. Leaflets are periodic images of the asymmetric lipid bilayer.

MOVIE S5.
Twinfilin tail in a β-sheet conformation does not bind the PI(4,5)P2-rich membrane leaflet efficiently (system 7). A simulation of twinfilin with the tail in a β-sheet conformation and membranes with (top) the PI(4,5)P2-rich and (bottom) the PI(4,5)P2-free leaflet. Leaflets are periodic images of an asymmetric lipid bilayer.

MOVIE S6.
Twinfilin tail in a α-helical conformation binds the PI(4,5)P2-rich membrane leaflet efficiently even without the ADF-H domain (system 9).

MOVIE S7.
Twinfilin without the tail does not bind the PI(4,5)P2-rich membrane leaflet (system 10). A simulation of twinfilin without its tail and membranes with (top) the PI(4,5)P2-rich and (bottom) the PI(4,5)P2-free leaflet. Leaflets are periodic images of an asymmetric lipid bilayer.

SUPPORTING REFERENCES

1. McGuffin, L. J., Bryson, K., and Jones, D. T. (2000) The psipred protein structure prediction server. *Bioinformatics* **16**, 404-405. 10.1093/bioinformatics/16.4.404
2. Yan, R., Xu, D., Yang, J., Walker, S., and Zhang, Y. (2013) A comparative assessment and analysis of 20 representative sequence alignment methods for protein structure prediction. *Sci. Rep.* **3**, e2619. 10.1038/srep02619
3. Drozdetskiy, A., Cole, C., Procter, J., and Barton, G. J. (2015) JPred4: A protein secondary structure prediction server. *Nucleic Acids Res.* **43**, W389-W394. 10.1093/nar/gkv332
4. Hartigan, J. (1975) Clustering Algorithms, J*ohn Wiley & Sons*, Inc. New York
5. Kalimeri, M., Rahaman, O., Melchionna, S., and Sterpone, F. (2013) How conformational flexibility stabilizes the hyperthermophilic elongation factor G domain. *J. Phys. Chem.* **117**, 13775-13785. 10.1021/jp407078z
6. Joosten, R.P., te Beek, T.A.H., Krieger, E., Hekkelman, M.L., Hooft, R.W.W., Schneider, R., Sander, C., Vriend, G., (2011) A series of PDB related databases for everyday needs. *Nucleic Acids Res.* **39**, D411–D419. 10.1093/nar/gkq1105
7. Kabsch, W., Sander, C., (1983) Dictionary of protein secondary structure: pattern recognition of hydrogen-bonded and geometrical features. *Biopolymers* **22**, 2577–2637. 10.1002/bip.360221211